Coral Reefs
October 2022, Volume 41, Pages 1611-1626
https://doi.org/10.1007/s00338-022-02319-7
https://archimer.ifremer.fr/doc/00799/91143/

A quick and cost-effective method for modelling water renewal in shallow coral reef lagoons

Lalau Noemie [1], Van Wynsberge Simon [1,*], Soulard Benoit [1], Petton Sébastien [1], Le Gendre Romain [2]

[1] Ifremer, UMR 9220 ENTROPIE (Institut de Recherche Pour le Développement, Université de la Réunion, Ifremer, Université de la Nouvelle-Calédonie, Centre National de la Recherche Scientifique), 98800, Nouméa, New Caledonia, France
[2] Ifremer, Univ. Brest, CNRS, IRD, LEMAR, 29840, Argenton, France

* Corresponding author : Simon Van Wynsberge, email address : Simon.Van.Wynsberge@ifremer.fr

Abstract :

Water renewal exerts a preponderant role in eutrophication, yet few hydrodynamic indicators exist for performing quick and cost-effective assessments of ecosystem vulnerability. Using field data, we closed the water budget of a shallow coral reef lagoon recently exposed to high levels of nutrient loading that triggered green tides. Then, we tested the relevance of modelling flushing-time, a proxy of water renewal, from oceanic and atmospheric open access data. Water inflows in the lagoon were mainly driven by waves breaking on exposed reefs, but tide and wind also influenced water renewal during low-wave periods. Modelling flushing-time as a function of the wave features (significant wave height, direction, and period), tide, and wind direction provided the most convincing model, with greater contribution of wave height, and adequately reproduced observations for an independent dataset. Using this model to hindcast flushing-time over the period 2000–2019 highlighted that green tides that recently struck the area in January 2018 and June 2019 followed periods of slow water renewal, which therefore contributed to amplify the blooms. The analysis also demonstrated that renewal events even slower than those recorded in 2018–2019 are frequent in this lagoon, which highlights the high vulnerability of this UNESCO World Heritage Site to other pulses of nutrient loading. Since the methodology developed in this study can be easily applied to many other coastal barrier and fringing reefs, it offers a promising perspective for quick and cost-effective assessments of coral reef vulnerability to eutrophication and other ecosystem crises magnified by slow water renewal.

Keywords : Coastal barrier reefs, Hydrodynamic indicators, Coral Reefs, Flush, Green tides, Eutrophication

Acknowledgements

We are grateful to R. Laigle, P. Laigle, G. Sarrailh, V. Bouvot, E. Le Tesson, J. Herlin, and C. Helleringer for their logistical support during fields trips, to J. Lefèvre for sharing personal data regarding water surface slope at PGD, and to two anonymous reviewers that made constructive comments on the manuscript. The study was funded by the ELADE project, with operating budget supported by La province Sud and salary budget supported by Ifremer (grant C.458-19).

Statements and Declarations

The authors have no competing interests to declare.

1. Introduction

As eutrophication is a problem of increasing importance in coral reef lagoons, new challenges are arising to assess the vulnerability of these ecosystems to nutrient inputs (Fabricius, 2011). Among these challenges is the identification of environmental conditions that put ecosystems at risk (Beroya-Eitner, 2016). Such vulnerability assessments are particularly useful for monitoring ecosystems affected by recurrent dystrophic events, determining the risk that another crisis may occur, and providing insights as to where and when more targeted policy interventions are necessary.

Water renewal is a key factor in eutrophication (Fabricius, 2011; Ferreira et al., 2011; Pinay et al., 2014; Schwichtenberg et al., 2017; Le Moal et al., 2019; Senent-Aparicio et al., 2021). Slow renewal of water in areas with elevated nutrient loads allows increasing exposure of algae to conditions propitious for growth (i.e., high levels of nutrients) and leads to higher primary production. Specifically for green tides, which refers to massive stranding of green macroalgae on beaches and stand among the many manifestations of eutrophication, slow renewal and high confinement of water masses are often mentioned as factors amplifying the extent of the blooms, when combined with nutrient enrichment (Ménesguen et al., 2010; Perrot et al., 2014; Ménesguen, 2018). In coral reefs, green tides are poorly documented, but it has been shown that slow renewal of water in lagoons leads to higher primary production (Andréfouët et al., 2001).

Many variables exist to quantify the renewal of water in coral reef lagoons (Jouon et al., 2006 ; Viero and Defina, 2016; Lucas and Deleersnijder, 2020). Among the most used are water export time or residence time, defined as the time taken by a particle, initially located at a given point, to leave the lagoon (Andréfouët et al., 2001; Jouon et al., 2006; Lucas and Deleersnijder, 2020); and “turnover time”, which is obtained by averaging residence time

over lagoon volume (Andréfouët et al., 2001). The residence time may vary inside the lagoon, whereas the "turnover time" is defined for the whole lagoon (Lucas and Deleersnijder, 2020). In the context of nutrient loading, the "e-folding flushing-time" and the "local e-folding flushing-time" are also highly relevant metrics, as they refer to the time needed to decrease a concentration of tracers by a factor $e = 2.718$. The e-folding flushing-time is relevant for the whole lagoon whereas the local e-folding flushing-time is a spatial variable relevant at intra-lagoon scale (Jouon et al., 2006). Computing these variables, however, require numeric modelling and particle tracking at high spatial resolution inside the lagoon. Drifters can be useful to estimate the residence time at a given location, date and time, but numerous drifters must be deployed concomitantly to provide an estimate of water renewal which is relevant at lagoon scale. This approach is too expensive to generate time series of water renewal, and cannot hindcast water renewal for past events during which no drifters were deployed. Although drifters can be used to validate hydrodynamic models, they cannot by themselves be used to estimate lagoon water renewal in a cost-effective way to assess lagoon vulnerability to eutrophication. Hydrodynamic models, in turn, require a detailed bathymetric map of the area, calibration/validation field data, advanced technical skills to set up or run the model, as well as heavy computing resources (Andréfouët et al., 2006a; Jouon et al., 2006; Umgiesser et al., 2014), and are currently only available for a handful of coral reef lagoons. When such models are available, outputs are provided for specific periods of interest and are not regularly updated, which limits the operability of using these metrics as indicator of ecosystem vulnerability in most coral reef lagoons.

A lower bound of the "turnover time" is the flushing-time, also named "renewal time" in the literature (Andréfouët et al., 2001, Lucas and Deleersnijder, 2020). The flushing-time is defined as the ratio between lagoon's volume and inflow or outflow of water, and converges to the "turnover time" under the assumption of a well-mixed lagoon (Monsen et al., 2002; Lucas and Deleersnijder, 2020). The flushing-time is a low-cost indicator of lagoon water renewal because if the inflow/outflow of water at the lagoon's border can be linked statistically to offshore forcings that are routinely accessible in near-real time from regional models, calculation of flushing-times can also be performed quickly and at reduced cost, without calling for intra-lagoon numeric modelling (Andréfouët et al., 2022).

Inflow and outflow of lagoon waters are primarily driven by tide, offshore waves, and wind, and reef geomorphology. Water inflow (through passes and above the barrier reef crest) is positive when ocean water level is above the lagoon water level, and negative otherwise (Lowe and Falter, 2015). The higher the offshore tidal

range, the stronger the water inflow and outflow to equilibrate the water levels between ocean and lagoon. Offshore sea state, either generated by distant storms or by local winds, can also enhance lagoon water renewal because high waves induce stronger fluxes above the reef edges (Massel and Gourlay, 2000; Lowe and Falter, 2015 ; Aucan et al., 2021). Wind also contributes to lagoon circulation by setting into motion the upper water layer and may influence water flow at lagoon borders (Tartinville et al., 1997; Deleersnijder, 2003; Dumas et al., 2012). To date, modelling lagoon flushing-time from regional open access data has only been done for atoll lagoons (Andréfouët et al., 2001; Andréfouët et al., 2022), using significant ocean wave height as the only forcing. The relevance of such approach for estimating water renewal for coastal lagoons remains to be demonstrated, and the variables to be included in the analysis must be clearly identified.

The present study focuses on the Poé-Gouaro-Déva (PGD) lagoon, New Caledonia. This area became part of the UNESCO's World Heritage List in 2008 and is currently one of the most recreational and touristic areas of Grande Terre (Fig. 1). Recently, high discharge of nutrients into the lagoon due to unreasonable use of fertilizers triggered outbreaks of the green algae, *Ulva batuffolosa* (Brisset et al., 2021; Lagourgue et al., 2022), resulting in mass stranding of algae on the beach in January 2018 and June 2019. These green tides raised sanitary concern and endangered touristic activities, important for the local economy. Local managers lacked information on the hydrodynamic conditions during and before the green tides; without this information, they cannot evaluate the likelihood that such events may occur in the future. In particular, it was unclear if the green tides resulted from high nutrient inputs only, or if the phenomenon was amplified by unusual conditions of slow lagoon water renewal. As with many other environmental crises in the South Pacific territories, answers were needed quickly and with restricted funding, and no 3D hydrodynamic model was available for this area at the time.

In this paper, we used a statistical modelling approach to hindcast PGD's lagoon flushing-time over the past decades from regional open access data. Specifically, we (i) used field data to close the lagoon water budget and calculate a flushing-time over a 5 months period; (ii) identified which forcing among wind, offshore waves and tide, drive lagoon water renewal and modelled statistically the flushing-time as a function of these variables; (iii) used this relationship to hindcast the flushing-times of the PGD lagoon over the 2000-2019 time frame, and assessed how unusual the flushing-times were when the 2018 and 2019 *Ulva* outbreaks occurred. Then, we discuss the value of modelling flushing-time from oceanic and atmospheric forcing in light of its use as indicator of lagoon vulnerability to eutrophication and discuss the feasibility of applying this approach to other coral reef lagoons.

2. Methods

A flowchart of the main steps implemented and data used in this study is provided in Fig. 2.

2.1. Study site

The main island of New Caledonia (Grande Terre) is located in the Pacific Ocean, 1,500 km east of Australia (Fig. 1a). It is surrounded by a 1,600 km long barrier reef, which delimits a 23,400 km² lagoon (Andréfouët et al., 2009). This study focuses on the Poe-Gouaro-Déva (PGD) area, on the West coast of Grande Terre, where the barrier reef complex lies directly in front of the coastline (Fig. 1b).

We here define the PGD lagoon as the shallow body of water (average depth at low tide: 1.5 m) that extends from the coastline to the reef crest, and is bordered in its northwestern part by a narrow but deep (20 m in average) break in the reef (locally named the "Sharks Fault"), and in its southeastern part by the Gouaro Bay. The delimited area (20,675,000 m²) is approximately rectangular, 10 km long and up to 3 km width (Fig. 1b). Within this lagoon, the substratum is mainly made up of sandy bottoms, sometimes covered by a diffuse seagrass bed. Reef flats surround the sandy terraces at the borders of the lagoon. A large (~ 9 km²) intermediate reef flat punctuated with coral patches also dominates the eastern part of the PGD lagoon. Finally, a fringing reef also borders the coastline over a width of several tens of meters, which is partially covered by a dense and multi-species seagrass meadow, composed of *Halodule uninervis*, *Thalassia hemprichii*, *Cymodocea rotundata*, *Cymodocea serrulate*, and *Halophila ovalis*. This seagrass bed, which stands among the widest of New Caledonia, is of high ecological significance (Payri et al., 2019).

Human population in the area has increased over the past decades, with 4,364 inhabitants counted for the municipality of Bourail in 1996 versus 5,531 in 2019. The main watershed is also subject to intensive agricultural and livestock activities. Urbanization, tourism activities, and agricultural plots are concentrated in the southeast of Shark Fault, facing the PGD lagoon. The Poé and Déva watersheds, which are among the main tourist hotspots of the territory, have undergone major changes over the last decade, with the number of houses doubling from 2002 to 2018, and the construction of a hotel complex, including a 100 ha Golf course, that started in 2013. All these activities contribute to lagoon eutrophication, but excessive use of fertilizers by the Golf course has been designated as the main cause of the 2018 green tide.

2.2. Field data acquisition and processing

Field data acquisition aimed at closing the water budget of the PGD lagoon by characterizing exchange dynamics on each lagoon border (west, east, and south lagoon sections, Fig. 1b). Note that field work did not aim at characterizing water circulation inside the lagoon, which is beyond the scope of this study.

Field missions were carried out to deploy the instruments during two periods: the first one from February to May 2019 (3 full months of measurements) and the second from July to September 2019 (2 full months). The first study period was affected by unusual extreme conditions from mid-February to early of March, generated by the tropical cyclone Oma that passed near the area. During this first period, 10 instruments were deployed. Eight current meters (MGL-JCU® Marotte HS) were deployed on the eastern reef flat (L01, L02, and L03), southern reef flat (L04, L05 and L06), and northwestern reef flat (L07 and L09). These tilt current meters are frequently used to measure currents in shallow waters (Page et al., 2021). Two 1 Hz RBR® temperature and depth loggers were deployed, at station O01 on the external reef slope at 10-m depth, and at L13 station inside the lagoon, respectively (Fig. 1b). These high-frequency time series of sea water level were processed to derive tidal, surge and sea-state signals (see below). During the second period, only the Marotte HS current meters were deployed. All metadata and data are available in open access (Le Gendre et al., 2020), and the exact positions, measurement types and frequency, mean depths, and deployment period of loggers are also provided in ESM_1.

All data processing has been done using Python software and packages. Tidal filtering (i.e., computation of surges) was achieved using Demerliac filter (Demerliac, 1974), and tidal harmonic decomposition (or recomposition) was performed on the basis of levels time series (at the hourly time step), using the solve and reconstruct functions within the Python utide tool, version 0.2.5. The methodology implemented by these functions are based on Codiga (2011). Wave parameters were computed from 1Hz level data using linear theory. Currents speed and direction were averaged hourly, since the very high frequency variability of water renewal was not the focus of this study. They were then projected on the normal to each section to obtain inflow/outflow speeds.

2.3. Calculating flushing-time from field data

We quantified the water renewal time of the PGD lagoon by using flushing-time. We calculated a "field" flushing-time (T_f) derived from hourly observations, as the ratio between the volume (in m^3) of the lagoon at time t (V_t) and the hourly flow of water (in $m^3\ h^{-1}$) leaving the lagoon at time t (Q_t) (eq. 1; Gallagher et al., 1971; Monsen et al., 2002; Lucas and Deleersnijder, 2020).

$$T_f = \frac{V_t}{Q_t} \qquad (eq.\ 1)$$

The higher T_f, the less efficiently the lagoon water is renewed. We used the volume of water leaving the lagoon to calculate T_f instead of using the volume of water entering the lagoon, since current meters captured the outgoing flow rate with more confidence than water flow entering the lagoon (see section 3.2). The volume of the lagoon at time t (V_t) was computed on the basis of lagoon surface area (A = 20,675,000 m²), averaged estimated bathymetry (H_0, Amrari et al., 2021) referenced vertically in line with the chart datum of Hydrographic Service of the French Navy, and measured water level (ξ_{obs} , eq. 2).

$$V_t = A \times (H_0 + \xi_{obs}) \qquad (eq.\ 2)$$

For water level, since a gap affected the L13 time series (ESM_1), we used water level measured at O01 instead. The validity of using O01 time series instead of L13 time series for calculating $\xi_{obs}$was checked by a sensitivity analysis, which highlighted negligible differences between T_f calculated with O01 and T_f calculated with L13 (ESM_2).

To calculate Q_t, time series of water levels were generated for each boundary section (west, east, and south sections, see Fig. 1b), from bathymetry and measured level variations in O01. Then, currents measured by the Marotte HS (C_t) were integrated over the cross-sectional area of height *h* and length *L* of each lagoon border (eq. 3). This calculation assumed a negligible surface slope inside the lagoon, which was verified *a posteriori* by 3D hydrodynamics model simulations, except during Oma at proximity of the reef crest (Lefèvre J., comm. pers.).

$$Q_t = \int_0^L (h(x) + \xi_{obs,t})\, dx \times C_t \qquad (eq.\ 3)$$

2.4. Offshore waves, offshore tide, and wind

To characterize offshore waves, the significant height of wind and swell waves (H_S^{ww3}), mean wave direction (θ^{ww3}) and peak period (T_p^{ww3}) were extracted from a WAVEWATCH III configuration over New Caledonia and Vanuatu (WW3, Rascle and Ardhuin, 2013). This product provides waves data every 3 hours at a 3 minutes spatial resolution (~ 5.5 km). Wave height values estimated by WW3 were validated for the PGD area using waves recorded by the pressure sensor at station O01 (see section 3.1).

For winds, ERA5 reanalysis (Hersbach et al., 2020) provides hourly wind velocities V^{era5} and direction θ^{era5} on a 30 km grid. Although ERA5 may not capture all wind patterns adequately at a very local scale, it is free of charge and available at global scale, thus fitted well the purpose of this study to validate a cost-effective proxy of water renewal that is adaptable for other reefs than PGD. For both WW3 and ERA5 products, data were extracted at the offshore gridpoint located the closest to the lagoon (long: 165.4°, lat: -21.65°). Considering tide (ξ), the field

observations in O01 allowed us to discriminate the main harmonic constituents and then to recompose hourly tidal dynamics at the desired period. Incident waves time series from WW3 have been interpolated at 1 hour frequency (spline interpolation) so that each dataset used for analyses is at a 1 hour time-step.

2.5. Modelling flushing-time from offshore waves, offshore tide, and wind

Given the non-linear relationship between flushing-time and forcing data, we expressed $\widehat{T_f}$ as a function of offshore waves (θ^{ww3}, H_s^{ww3} and T_p^{ww3}), tide (ξ), and winds (V^{era5} and θ^{era5}), on the basis of generalized additive models (GAM; eq. 4) using the GammaGAM function provided by Python package Pygam version 0.8.0 (see Servén & Brummitt, 2018).

$$\widehat{T_f} = s(\theta^{ww3}) + s(H_s^{ww3}) + s(T_p^{ww3}) + s(\xi) + s(V^{era5}) + s(\theta^{era5}) + \beta \qquad \text{(eq. 4)}$$

Where s( ) refers to smoothing functions and β the intercept. Since events of slow water renewal (i.e., longer flushing-time) were of greater concern than faster flushing-times in the context of *Ulva* sp. blooms at PGD, the statistical relationship was calibrated for the post-cyclone period only (from 04/03/19 to 30/04/19) to avoid overdriving smoothing functions by extreme conditions that generate fast flushing-times. Pearson correlations between input variables were performed, and the latter were added one by one in the model to avoid overfitting the model with correlated variables (Larsen, 2015). Variables were added in the model following this order: θ^{ww3}, H_s^{ww3}, ξ, θ^{era5}, V^{era5}, and T_p^{ww3}. Wave direction and height (θ^{ww3} and H_s^{ww3}) were first added as it was evident from data that they were the most important factors influencing current speed recorded by tilt current meters (see result section). Wave period (T_p^{ww3}), wind speed (V^{era5}) and wind direction (θ^{era5}) were correlated with wave features already included in the model (Pearson correlations from 0.32 to 0.73), and were thus the last variables added. At each step, models were compared using Akaike Information Criterion (AIC); Complexified models that decreased AIC by more than 2 units were considered supported, following Burnham & Anderson (2002). The best model (i.e., model with the lowest AIC) was used for further analyses (see next section). The contribution of each parameter into the best model was further evaluated using p-value provided by the summary function of package Pygam.

The ability of the statistical model to predict flushing-times accurately was evaluated using an independent data set. For this, we used the second period of field observations (i.e., from 01/07/19 to 01/09/19). Fitted values of

flushing-time ($\widehat{T_f}$) were compared to observations (T_f) using a coefficient of determination denoted R^2 and calculated as:

$R^2 = \frac{\sum(T_f - \hat{T}_f)^2}{\sum(T_f - \overline{T_f})^2}$ (eq. 5)

Where overbar represents overall mean.

2.6. Hindcast of flushing-times over the past decades

The best model previously validated was used to assess the range of flushing-times that characterized the PGD lagoon from January 2000 to December 2019. First, modelled flushing-times ($\widehat{T_f}$) over the 2000-2019 period were averaged by month, and monthly anomalies were computed for each month *m* and year *y*, following eq. 6.

$A_{m,y} = \overline{\widehat{T_f}_{m,y}} - \overline{\widehat{T_f}_{m,2000-2019}}$ (eq. 6)

Where $\overline{\widehat{T_f}_{m,y}}$ is the mean flushing-times computed for a given month *m* and year *y*, and $\overline{\widehat{T_f}_{m,2000-2019}}$ is the average flushing-times of month *m* over the 2000 – 2019 timeframe.

Second, we found the number of slow renewal events that occurred for each month of the 10-year period. For this, a slow renewal event had a peak flushing-time > 30.4 hr, which corresponds to the mean plus three units of standard deviation of $\widehat{T_f}$ over the period 2000-2019.

Hindcast time series of flushing-times and number of slow renewal events were used to assess how unusual the flushing-times were when the 2018 and 2019 *Ulva* outbreaks occurred.

3. Results

3.1. Wind, offshore waves, and offshore tide

Wind parameters extracted from ERA 5 highlighted that the PGD area was dominated by relatively strong (6 m s^{-1} on average) southeastern trade winds during the two periods of measurements (Fig. 3a and ESM_3). These trade winds were modulated by daily variations with a minimum at night, followed by a maximum during the day and a fall at the end of the afternoon (Fig. 3a, blue lines). This wind pattern is representative of the most dominant pattern that characterizes New Caledonia through the year (Lefèvre et al., 2010). During the period influenced by Oma, wind patterns that affected the PGD area shifted from moderate trade winds to northerly winds and finally strong southeast winds at the climax of the event, with a maximum velocity of 17 m s^{-1} (Fig. 3a).

Waves remained of moderate height, usually bellow 2.5 m, during the two periods of measurements, with a direction between 160 and 220°. However, each of the two deployment periods experienced a large wave event.

The first was caused by Oma with H_s reaching up to 6m around 25/02/19 and the second occurred around 22/08/19 due to remotely-generated swells (H_s up to 5m and period around 15s, see ESM_3). Mean wave peak period (T_p) ranged between 6 s and 17 s during the first period of measurement, and between 8 s and 18 s during the second period of measurement. Although slightly overestimated when not from the S-SE, significant wave height simulated with WW3 was generally congruent with significant wave height measured with RBR sensors (Fig. 3b), with a mean difference between the two variables of 0.38 m and a Pearson correlation coefficient of 0.95. Similarly, T_p simulated with WW3 was usually congruent with T_p measured from RBR sensor (mean difference between T_p^{ww3} and T_p^{RBR} = -0.64 s and Pearson correlation = 0.75 ; Fig. 3b).

Tide followed a micro-tidal, mixed and mainly semi-diurnal pattern (Fig. 3c; Douillet, 1998), with offshore sea height variation due to tide (ξ) ranging between -0.76 m and 0.74 m during the two periods of measurements. Minimal tidal ranges during neap tides were 0.59 m and 0.67 m during the first and during the second periods of measurements, respectively. Tidal range reached 1.48 m during spring tides of the two periods.

Correlation between forcing variables were weak (Table 1), except between wind speed (V^{era5}) and wave height (H_s^{ww3}; r = 0.73), as well as between wind direction (θ^{era5}) and wave direction (θ^{ww3}; r = 0.52).

3.2. Inflows and outflows at lagoon borders

The analysis of offshore waves, offshore tide, and current data at lagoon borders highlighted that water inflows were mainly driven by offshore waves breaking on the southern reef crest (Fig. 3b; 3d), while outflows occurred through the Sharks Fault in the western part of the PGD lagoon, and toward the Gouaro Bay in its eastern part (Fig. 3d). Along the southern reef, the mean current flow was consistently into the lagoon, whereas the mean flows at the eastern and western reef edges were mostly directed out of the lagoon (outflows, Fig. 3d). At these eastern and western lagoon borders, inflows were only recorded 5 % of the time (on average, a cumulative total of 1.3 hr d^{-1}). Current meter L04 was more sheltered from offshore waves than L05 and L06, and displayed lower speed flows. The hourly-averaged current magnitudes along the eastern reef edge were well correlated (ESM_4), with Pearson correlation between sensors ranging from 0.86 to 0.96 for speed. Current measurements taken along the eastern reef edge had uniform direction 91% of time. The current magnitudes along the western reef edge near the Sharks Fault were also well correlated (ESM_5), with Pearson correlation of 0.81 for speed, and 96% of time current measurements taken along the western reef edge had uniform direction.

During low wave episodes, tide could also influence flows at lagoon's borders. At the eastern and western reefs stronger outflow occurred at ebb tide (Fig. 4a and 4b), but reduced outflow and occasional inflow could occur during rising tide. Inflows at the east and west sections of the lagoon occurred only during spring tides coinciding

with low waves (Fig. 3b-d) and were restricted to short pulses, especially near the shore (ESM_4). Wind appears to play a less prominent role than waves and tide in the dynamics of inflows and outflows at lagoon borders (Fig. 3a, 3d, and 4e-f), nevertheless strong winds co-occur with strong outflows, and inflows at the east and west sections never occurred during periods of strong winds.

3.3. Observed and modelled flushing-times

Flushing-time as calculated from field data (T_f) ranged between 4 hr and 29.5 hr during the two periods of measurements (mean ± standard deviation: 10.75 ± 4.75). Notably, three long flushing-time events (T_f = 27.7, 28.9, and 29.5 hr) were recorded during the first period of measurements, on the 07/03/19, 18/03/19, and 23/03/19, respectively (Fig. 5a).

Modelling flushing-time as a function of wave direction (θ^{ww3}), wave height ($H_S{}^{ww3}$), tide (ξ), wind direction (θ^{era5}), and mean wave peak period ($T_p{}^{ww3}$), provided the most convincing model (Table 2). Adding wind speed (V^{era5}) in the model increased AIC (AIC = 9146 for model 5 compared to 9117 for model 4), thus this parameter was not retained. The best model (i.e., model 6, Table 2) explained 86 % of T_f's variance over the calibration data set (i.e., first period of measurements), with much greater contribution of $H_S{}^{ww3}$ ($p < 0.001$) compared to θ^{era5} ($p = 0.25$), θ^{ww3} ($p = 0.33$), ξ ($p = 0.44$), and $T_p{}^{ww3}$ ($p = 0.76$; Table 3).

Overall, model 6 performed well in estimating the flushing-time of PGD's lagoon using an independent dataset, with 90 % of T_f's variance explained by $\widehat{T_f}$ over the second period of measurements (Fig. 5b). Significant differences between observations and predictions of flushing-times nevertheless occurred occasionally. Notably, this included a 4 hr underestimation of flushing-time by the model during a low-wave and low-wind period around the 13/07/19, and a 3 hr overestimation of flushing-time by the model around the 23/07/19 during a period of SE waves. Conversely, the highest values of $H_S{}^{ww3}$ were recorded around the 22/08/19, while no event of this magnitude was found during the period used for model calibration, leading to a wide confidence interval around model prediction for this period (Fig. 5b and ESM_3).

3.4. Hindcast of flushing-times over the past decades

The median flushing-time over the period 2000-2019 was 9.7 hr, meaning that the PGD lagoon typically renews its entire volume of water between two and three times a day. A seasonal trend affected the flushing, with longer flushing-times hindcasted in December (14.0 hr ± 2.4 sd), and faster flushing-times hindcasted in July (9.1 hr ± 1.4 sd). The stranding of green algae that were observed on PGD's beaches in January 2018 followed three long

flushing-time events, respectively occurring on 31/12/17 with $\widehat{T_f}$ = 32 hr [IC95% 10 – 110 hr], on 01/01/18 with $\widehat{T_f}$ = 34 hr [IC95% 17 – 72 hr], and on 15/01/18 with $\widehat{T_f}$ = 34 hr [IC95% 24 – 48 hr] (Fig. 6a), and the green tide that occurred in June 2019 followed one long flushing-time event with $\widehat{T_f}$ = 31 hr [IC95% 23 – 42 hr] (Fig. 6b). The slowest water renewal was hindcasted for January 2002, with flushing-time up to 3 days ($\widehat{T_f}$ = 71 hr [IC95% 35 – 146 hr]). The number of slow renewal events was lower from 2017 to 2019 than earlier in the decade (Fig. 6d). Notably, up to 30 slow water renewal events were hindcasted in January 2004.

4. Discussion

4.1. Offshore waves as main driver of water renewal

In the PGD lagoon, offshore waves were the predominant forcing that drove water renewal, with faster renewal during periods of high waves, and slow renewal during low wave periods. Water inflows across the reef were generated by incident waves with outflows occurring at the east and west lagoon sections, which are more sheltered from waves and where topography offers pathways for outgoing fluxes. This pattern of in/out flows is typical of many coral reef lagoons (Callaghan et al., 2006; Taebi et al., 2011; Lowe and Falter, 2015; Storlazzi et al., 2018), and has previously been used to estimate flushing-time in Tuamotu atolls (Andréfouët et al., 2001; Andréfouët et al., 2022). Since the height of offshore waves is available routinely from regional oceanic models, Andréfouët et al. (2001) extrapolated their relationship for a panel of atoll lagoons and highlighted good correlation between long flushing-time and phytoplankton concentration in lagoons. This wave-based approach was only justified for atolls in the Tuamotu Archipelago because they are affected by low tidal ranges (i.e., ~ 1 m during spring tides). In these closed systems, wind and tide can drive circulation of lagoons (Deleersnijder, 2003; Dumas et al., 2012), but their influence on water exchanges between lagoon and ocean are usually negligible compared to waves. In our study, we demonstrate that wave height was the main contributor of water renewal in a coastal barrier reef. However, we also highlight that statistical models of flushing-time lose significant information if they are only based on waves, with much lower AIC for model 3 (which include tide) compared to model 2 (which does not; ΔAIC = 114), and slightly, but significantly lower AIC for model 4 (which include wind direction) compared to model 3 (which does not; ΔAIC = 5; see Table 2). Tide at PGD is nearly two times greater than in Tuamotu archipelago (tidal range in PGD ~1.45 m *versus* 0.8 m in the middle of Tuamotu), and wind is also more variable in the west coast of New Caledonia (Lefèvre et al., 2010 ; Dutheil et al., 2020). As a result, wind and tide at PGD were worth taking into account for modelling flushing-time, as they could influence inflows and outflows at lagoon

borders during periods of low waves. We thus advocate for taking tide and wind forcings into account when estimating flushing-time in coral reefs, except when there is strong evidence that these factors can be neglected. Interestingly, tide has been identified as an important driver of water inflows within the Ouano lagoon, located ~50 km South-East of PGD (Chevalier et al., 2015; Sous et al., 2017). The contrast in forcing variables at Ouano (mainly tide driven) compared to PGD (mainly wave driven) despite their geographic proximity could have resulted from the presence of two wide and deep reef openings toward ocean at Ouano, as well as from differences in geomorphology between the two lagoons. Indeed, shallow terraces (< 4 m depth) of the coastal barrier reef complex lie directly in front of the shore at PGD, whereas they are separated from the shore by a deeper lagoon (~10 m deep) at Ouano. In the latter case, defined as a "channel lagoon" by Sous et al. (2017), current speed and direction on the barrier reef flats and terraces were driven by wave setup and breaking on reef crests, but tide drives inflows and outflows through the wide reef passes and therefore played a major role in lagoon water renewal (Chevalier et al., 2015). For the purpose of estimating water renewal, we advocate that shallow coastal barrier reefs characterized by shallow depth from shore to outer reef and negligible inflows through nearby reef passes or lagoon borders (like in the PGD lagoon) should be distinguished from "channel lagoons" (sensus Sous et al., 2017, like the Ouano lagoon), because the main drivers of water renewal (i.e., factors that must be integrated in the analysis) differ between the two types.

4.2. Relevance of the approach for other coral reef ecosystems

The PGD lagoon is characterized by a number of specificities that justified the methodology used in our study to calculate and model water renewal, but may limit its transposition to some other reef configurations without any adaptation. First, owing to its small area and depth, the PGD lagoon was deemed sufficiently well-mixed. This hypothesis was supported by numerous CTD profiles performed in this area, which highlighted no vertical stratification, with a maximum difference of 0.00216 kg m^{-3} between density at 0.5 m and density at the sea bottom (Brisset M. pers. com.). These characteristics justified the use of the flushing-time as proxy of water renewal in our study, because the flushing-time is equal to the "turnover time" only if the time scale of mixing inside the lagoon is much lower than the time scale for exchanges with the ocean (Andréfouët et al., 2001). The same hypothesis can nevertheless be applied to many shallow coastal barrier reef complexes and fringing reefs worldwide, which are usually smaller in size and shallower than the PGD lagoon (Andréfouët et al., 2006b). However, for lagoons that are not as well mixed as in our case study, using the flushing-time as proxy of lagoon water renewal is not recommended (Monsen et al., 2002; Lucas and Deleersnijder, 2020). Such configuration is

sometimes encountered in deep and/or highly reticulated lagoons (Schlager & Purkis, 2014; Andréfouët et al., 2020), in reefs composed of various geomorphological units, with some of them being more connected to ocean than others (Storlazzi et al., 2018), or in lagoons affected by thermal stratification. Applying a similar modelling approach as in our study to a lagoon punctually affected by thermal stratification calls for a preliminary analysis to check that mixing inside the lagoon remains sufficiently high compared to exchanges with the ocean.

Second, the morphology of the PGD lagoon and patterns of inflows/outflows at its borders facilitated the calculation of flushing-time. Indeed, the PGD lagoon is of rectangular shape bordered by continuous reefs, with the main inflows occurring uniformly across the southern reef, and outflows uniformly across the eastern and western extremities of the lagoon (Fig. 1; 3d; and ESM_4 and ESM_5). This pattern of inflows and outflows allowed us to calculate T_v on the basis of averaged outflows across the east and west lagoon sections (eq. 3). This straightforward approach for estimating flushing-time remains relevant for many coral reefs, since the circulation pattern at PGD is classical of coastal barrier reef complexes and fringing reefs (Taebi et al., 2011; Chevalier et al., 2015; Sous et al., 2017). In some reefs, however, inflows across reef edges can be intertwined with other patterns driven by specific wave, tide and wind conditions (Lindhart et al., 2021), or locally affected by small scale features. For such specific systems, our approach remains relevant to estimate water renewal at lagoon scale, provided that current speed and direction are measured using a comprehensive sampling scheme and during a period long enough to capture the spatio-temporal variability of inflows and outflows. Notably, calculation of the flow of water leaving/entering the lagoon (Q_t) and ultimately flushing-time (eq. 1 and 3) must be addressed at a resolution that allows depicting adequately inflows from outflows, otherwise flushing-time estimates might be biased. To this purpose, since Q_t can be calculated either from inflows or from outflows, we recommend using the flow whose variability is better captured by the sampling scheme.

As long as the conditions mentioned above are met, the approach developed in this study to model flushing-time remains compatible with other coastal barrier reef complexes and with island or continental fringing reefs. Notably, coastal barrier reef complexes are found in the Society archipelago, French Polynesia (e.g., Moorea, Maiao, and west coast of Tahiti, Andréfouët et al., 2006b), and island or continental fringing reefs are found for instance in Samoa, Fidji, Vanuatu, La Réunion and Mauritius islands, Guam, and along the west coast of Australia (Andréfouët et al., 2006b; Monismith et al., 2013 ; Pequignet et al., 2014). The quick and cost-effective approach developed here to measure then model flushing-time thus offers promising perspectives to characterize and hindcast lagoon water renewal regimes for a variety of coral reefs worldwide.

4.3. Values of the approach for managing the risk of eutrophication in coral reefs

The statistical approach performed in this study allowed us to estimate the range of flushing-times that characterized the PGD lagoon over the past two decades, including before the green tide events that hit PGD's beaches in 2018 and 2019. Specifically, we provided evidence that the PGD lagoon is usually well flushed, with an average flushing-time of 9.7 hr over the 2000-2019 period. Assuming well-mixed lagoon water, this means that the PGD lagoon entirely renews its waters 2-3 times a day on average. During low wave episodes, flushing-time increased significantly. The two green algae beach stranding events that occurred in January 2018 and June 2019 followed periods of slow water renewal that may have contributed in amplifying the algal blooms. Notably, three long flushing-time events preceded the January 2018 green tide (Fig. 6a). The green tide that occurred on 01/06/19, smaller in extent compared to the first event, also followed one long flushing-time event (Fig. 6b). The benthic green macroalgae were removed from their substrate by high swell from south west (making the report of algae on the beach concomitant with fast flushing time), but these slow renewal events certainly contributed to their growth considering the time scale of *Ulva* dynamics (Sun et al., 2020). Although these long flushing-time events (i.e., slow renewal of lagoon water) were among the longest recorded between 2017 and 2019, they were not unusual for the PGD lagoon (Fig. 6c and 6d). Specifically in January 2002, an event of slow water renewal was hindcasted, with flushing-time up to 71 hr [IC95% 35 – 146 hr]. In fact, 2017 was quite unusually highly flushed compared to usual conditions, as shown by negative monthly flushing anomalies hindcasted for this year (Fig. 6c). Slow renewal events were also few, with only one event recorded in December 2017 and two events recorded in January 2018 before the green tide. Such events have been much more numerous during the past decades, with up to 30 events in January 2004 (Fig. 6d). These results highlight strong vulnerability of the PGD lagoon to macroalgae blooms in case of other pulses of nutrient inputs. This is important information for local managers as it provides evidence that the green tides reported at PGD in 2018 and 2019 cannot be attributed to unusual conditions of slow lagoon water renewal, and that high nutrient inputs is the main factor that triggered the phenomenon.

Beyond assessing the risk of green tides, future work may attempt to predict the extent and longevity, and time of dissipation of blooms. These variables, however, strongly depend on other factors than flushing (e.g., swell and wind that pull algae from their substrate; duration and intensity of nutrient load; time series of light intensity at lagoon bottom). Like for most coral reefs worldwide, such detailed environmental data are not yet available nor modelled for the PGD lagoon. Predicting the dynamics of macroalgae blooms requires data to characterize all the processes that influence green algae dynamics, but also more data regarding the extent, duration, and longevity of green algae blooms than are currently available, to validate the models. The abundance of algae can to some extent

be hindcasted by remote sensing (Brisset et al., 2021), but this tool cannot yet be used to characterize extent, duration, and longevity of the blooms with sufficient resolution due to the frequency of this remote sensing data (> 5 days). Note that the aim of this study was to assess the value of modelling flushing time from oceanic and atmospheric forcing in light of its use as indicator of lagoon vulnerability to eutrophication, not to predict macroalgae biomass.

Beyond our green tide case study, we here demonstrate the value of statistically modelling lagoon flushing-time from oceanic and atmospheric forcing, which provide a cost-effective approach to assess lagoon vulnerability to eutrophication or other types of ecosystem crisis triggered or magnified by slow water renewal (Fabricius, 2011; Pinay et al., 2014; Andréfouët et al., 2014). The approach developed here balances the lagoon water budget by measuring inflows and outflows using a set of sensors deployed at lagoon's borders only, and is, to our knowledge, performed here for the first time in a coastal coral reef lagoon. The strength of this approach relies in the fact that an extensive characterization of water circulation inside the lagoon and its driving factors is not necessary to calculate flushing-times, and thus requires few numeric resources compared to 3D numeric modelling of hydrodynamics (Jouon et al., 2006). Time lags are not considered in the statistical model that link oceanic forcings and flushing-time, but such time lags appeared to be negligible at PGD owing to its small surface area and shallow depth. Numeric models can better take the non-linearity of physical processes into account, provide a spatial view of intra-lagoon variability which is of great value for tracking the path of nutrients, and can also quantify flow re-entrainment (i.e., amount of water exiting the lagoon that recirculate back into the reef system) with better accuracy than statistical models (Winter et al., 2020). However, for many lagoons like PGD no 3D hydrodynamic model exists at a satisfying spatial resolution. The numeric approach thus requires setting up a new configuration, which requires specific expertise and is much more time consuming than the statistical approach developed in this study. The numeric approach also requires bathymetric data of high quality and at high spatial resolution, which is currently lacking for many coral reefs. Where 3D hydrodynamic models validated at lagoon scale are available, outputs are not provided in near real-time which limit their interest to provide operational indicators for ecosystem monitoring. Model outputs can nevertheless be very useful to validate underlying hypotheses assumed when using flushing-time as a proxy of water renewal. Although the statistical approach does not replace hydrodynamic numeric modelling, it provided reliable estimates of flushing-times for the PGD lagoon at reduced cost and computing time. For quick and cost-effective identification of ecosystem vulnerability in lagoons where 3D

numeric modelling is not yet validated or available in near real-time with sufficiently good resolution, such approach is therefore very attractive.

5. Conclusion

In this study, we adopted a statistical approach to estimate the flushing-time of a shallow wave-driven lagoon, by combining field data and data extracted from regional models available in near-real time. The statistical model used in this study to hindcast the long-term dynamics of flushing-times required few resources compared to numeric modelling of hydrodynamics yet was useful for managing the risk of eutrophication in the PGD lagoon. It confirmed that the two green tide events that occurred in 2018 and 2019 followed periods of slow water renewal, which allowed the algae biomass to amplify during these periods of high nutrient discharge. The statistical modelling approach also evidenced that such periods of slow water renewal are frequent in the PGD lagoon, and that events of slow flushing even more intense than those recorded in 2018-2019 can frequently affect this lagoon. This points out the high vulnerability of this lagoon to green tides, and demonstrates the value of statistically modelling lagoon flushing time to assess lagoon vulnerability to eutrophication. The methodology developed here was well adapted for the PGD case study, but can be translated to many other coastal barrier reefs and fringing reefs. Overall, this approach offers promising perspectives for quick and cost-effective assessment of ecosystem vulnerability in coral reefs where eutrophication and other ecosystem crises are magnified by slow water renewal.

References

Amrari S, Bourassin E, Andréfouët S, Soulard B, Lemonnier H, Le Gendre R (2021) Shallow water bathymetry retrieval using a band-optimization iterative approach: application to New Caledonia coral reef lagoons using Sentinel-2 data. Remote sensing 13(20): 4108. https://doi.org/10.3390/rs13204108.

Andréfouët S, Pagès J, Tartinville B (2001) Water renewal time for classification of atoll lagoons in the Tuamotu Archipelago (French Polynesia). Coral Reefs 20: 399-408.

Andréfouët S, Ouillon S, Brinkman R, et al. (2006a) Review of solutions for 3D hydrodynamic modelling applied to aquaculture in South Pacific atoll lagoons. Marine Pollution Bulletin 52(10): 1138-1155.

Andréfouët S, Muller-Karger FE, Robinson JA, Kranenburg CJ, Torres-Pulliza D, Spraggins SA, Murch B (2006b) Global assessment of modern coral reef extent and diversity for regional science and management applications: a view from space. In Proceedings of the 10th International Coral Reef Symposium 2: 1732-1745.

Andréfouët S, Cabioch G, Flamand B, Pelletier B (2009) A reappraisal of the diversity of geomorphological and genetic processes of New Caledonian coral reefs: A synthesis from optical remote sensing, coring and acoustic multibeam observations. Coral Reefs 28: 691-707.

Andréfouët S, Dutheil C, Menkes C, Bador M, Lengaigne M (2014) Mass mortality events in atoll lagoons: environmental control and increased future vulnerability. Global Change Biology 21(1): 195-205. https://doi.org/10.1111/gcb.12699.

Andréfouët S, Genthon P, Pelletier B, Le Gendre R, Friot C, Smith R, Liao V (2020) The lagoon geomorphology of pearl farming atolls in the Central Pacific Ocean revisited using detailed bathymetry data. Marine Pollution Bulletin 160: 111580.

Andréfouët S, Desclaux T, Buttin J, Jullien S, Aucan J, Le Gendre R, Liao V (2022) Periodicity of wave-driven flows and lagoon water renewal for 74 Central Pacific Ocean atolls. Marine Pollution Bulletin 179: 113748.

Aucan J, Desclaux T, Le Gendre R, Liao V, Andréfouët S (2021) Tide and wave driven flow across the rim reef of the atoll of Raroia (Tuamotu, French Polynesia). Marine Pollution Bulletin 171: 112718.

Beroya-Eitner MA (2016) Ecological vulnerability indicators. Ecological Indicators 60: 329-334.

Brisset M, Van Wynsberge S, Andréfouët S, Payri C, Soulard B, Bourassin E, Le Gendre R, Coutures E (2021) Hindcast and near real-time monitoring of green macroalgae blooms in shallow coral reef lagoons using sentinel-2: A New-Caledonia case study. Remote Sensing 13(2): https://doi.org/10.3390/rs13020211.

Burnham KP, Anderson DR (2002) In: Model selection and multimodel inference. Practical Use of the Information-Theoretic Approach, second edition: 75-117. Springer-Verlag, New York, USA.

Callaghan DP, Nielsen P, Cartwright N, Gourlay MR, Baldock TE (2006) Atoll lagoon flushing forced by waves. Coastal Engineering 53: 691-704.

Chevalier C, Sous D, Devenon JC, Pagano M, Rougier G, Blanchot J (2015) Impact of cross-reef water fluxes on lagoon dynamics: a simple parameterization for coral lagoon circulation model, with application to the Ouano lagoon, New Caledonia. Ocean Dynamics 65: 1509-1534.

Codiga DL (2011) Unified Tidal Analysis and Prediction Using the UTide Matlab Functions. Technical Report 2011-01. Graduate School of Oceanography, University of Rhode Island, Narragansett, RI: 59pp. ftp://www.po.gso.uri.edu/ pub/downloads/codiga/pubs/2011Codiga-UTide-Report.pdf

Deleersnijder E (2003) Comments on "Water renewal time for classification of atoll lagoons in the Tuamotu Archipelago (French Polynesia)" by Andréfouët et al. [Coral Reefs (2001) 20:399-408]. Coral Reefs 22 : 307-308.

Demerliac A (1974) Calcul du niveau moyen journalier de la mer. Rapport du service hydrographique de la marine 741: 49–57.

Douillet P (1998) Tidal dynamics of the south-west lagoon of New Caledonia: observations and 2D numerical modelling. Oceanologica Acta, 21(1): 69-79.

Dumas F, Le Gendre R, Thomas Y, Andréfouët S (2012) Tidal flushing and wind driven circulation of Ahe atoll lagoon (Tuamotu Archipelago, French Polynesia) from *in situ* observations and numerical modelling. Marine Pollution Bulletin 65 (10-12): 425-440.

Dutheil C, Andréfouët S, Jullien S, Le Gendre R, Aucan J, Menkes C (2020) Characterization of south central Pacific Ocean wind regimes in present and future climate for pearl farming application. Marine Pollution Bulletin 160: 111584.

Fabricius KE (2011) Factors Determining the Resilience of Coral Reefs to Eutrophication: A Review and Conceptual Model. Coral Reefs: An Ecosystem in Transition: pp 493-505.

Ferreira JG, Andersen JH, Borja A, Bricker SB, Camp J, da Silva MC, Garcés E, Heiskanen AS, Humborg C, Ignatiades L, Lancelot C, Menesguen A, Tett P, Hoepffner N, Claussen U (2011) Overview of eutrophication indicators to assess environmental status within the European Marine Strategy Framework Directive. Estuarine, Coastal and Shelf Science 93 (2): 117-131.

Gallagher BS, Shimada KM, Gonzales FI, Stroup ED (1971) Tides and currents in Fanning atoll lagoon. Pacific Science 25:191-205.

Hersbach H, Bell B, Berrisford P, et al. (2020) The ERA5 global reanalysis. Quarterly Journal of the Royal Meteorological Society 146(730): 1999-2049.

Jouon A, Douillet P, Ouillon S, Fraunié P (2006) Calculations of hydrodynamic time parameters in a semi-opened coastal zone using a 3D hydrodynamic model. Continental Shelf Research 26 (12-13): 1395-1415.

Lagourgue L, Gobin S, Brisset M, Vandenberghe S, Bonneville C, Jauffrais T, Van Wynsberge S, Payri C (2022) Ten new species of Ulva (Ulvophyceae, Chlorophyta) discovered in New Caledonia: Genetic and morphological diversity, and bloom potential. European journal of Phycology: 1-21. https://doi.org/10.1080/09670262.2022.2027023.

Larsen K (2015) GAM: the predictive modelling silver bullet. Multithreaded. Stitch Fix, 30: 1-27.

Lefèvre J, Marchesiello P, Jourdain NC, Menkes C, Leroy A (2010) Weather regimes and orographic circulation around New Caledonia. Marine Pollution Bulletin 61 (7-12) : 413-431.

Le Gendre R, Soulard B, Lalau N, Bruyere O, Van Wynsberge S (2020) Field observations of Hydrodynamics in a shallow coral reef lagoon : Poe lagoon - New Caledonia. SEANOE. https://doi.org/10.17882/76334.

Le Moal M, Gascuel-Odoux C, Ménesguen A, Souchon Y, Etrillard C, Levain A, Moatar F, Pannard A, Souchu P, Lefebvre A, Pinay G (2019) Eutrophication: A new wine in an old bottle? Science of the Total Environment 651: 1-11.

Lindhart M, Rogers JS, Maticka SA, Woodson CB, Monismith SG (2021) Wave modulation of flows on open and closed reefs. Journal of Geophysical Research: Oceans 126: e2020JC016645.

Lowe RJ, Falter JL (2015) Oceanic Forcing of Coral Reefs. Annual Review of Marine Science 7: 43-66.

Lucas LV, Deleersnijder E (2020) Timescale methods for simplifying, understanding and modeling biophysical and water quality processes in coastal aquatic ecosystems: a review. Water 12(10): 2717.

Massel SR, Gourlay MR (2000) On the modelling of wave breaking and set-up on coral reefs. Coastal Engineering 39(1): 1-27.

Ménesguen A, Perrot T, Dussauze M (2010) Ulva Mass Accumulations on Brittany Beaches: Explanation and Remedies Deduced from Models. Mercator Ocean Quarterly Newsletter, 38: 4-13.

Ménesguen A (2018) Les Marées Vertes. 40 Clés Pour Comprendre; Edition Quae: Versailles, France: pp 119.

Monismith SG, Herdman LMM, Ahmerkamp S, Hench JL (2013) Wave transformation and water-driven flow across a steep coral reef. Journal of Physical Oceanography 43(7): 1356-1379.

Monsen N, Cloern JE, Lucas L, Monismith SG (2002) A comment on the use of flushing-time, residence time, and Age as transport time scales. Limnology and Oceanography 47 (5): 1545-1553. https://doi.org/10.4319/lo.2002.47.5.1545.

Page CE, Leggat W, Heron SF, Fordyce AJ, Ainsworth TD (2021) High flow conditions mediate damaging impacts of sub-lethal thermal stress on corals' endosymbiotic algae. Conservation Physiology 9(1): coab046.

Payri CE, Allain V, Aucan J, David C, David V, Dutheil C, Loubersac L, Menkes C, Pelletier B, Pestana G, Samadi S (2019) New Caledonia. In World Seas: An Environmental Evaluation Chapter 27: 593-618.

Péquignet ACN, Becker JM, Merrifield MA (2014) Energy transfer between wind waves and low-frequency oscillations on a fringing reef, Ipan, Guam. JGR Oceans 119(10): 6709-6724.

Perrot T, Rossi N, Ménesguen A, Dumas F (2014) Modelling green macroalgae blooms on the coasts of Brittany, France to enhance water quality management. Journal of Marine Systems 132: 38-53.

Pinay G, Gascuel C, Ménesguen A, Souchon Y, Le Moal M (coord), Levain A, Etrillard C, Moatar F, Pannard A, Souchu P (2014) L'eutrophisation: manifestations, causes, conséquences et prédictibilité. Synthèse de l'Expertise scientifique collective CNRS – Ifremer - INRA – Irstea (France) : 148 pages.

Rascle N, Ardhuin F (2013) A global wave parameter database for geophysical applications. Part 2: Model validation with improved source term parameterization. Ocean Modelling 70: 174-188.

Schlager W, Purkis S, (2014) Reticulated reef patterns – antecedent karst versus self-organization. Sedimentology 62: 501-515.

Schwichtenberg F, Callies U, van Beusekom JEE (2017) Residence times in shallow waters help explain regional differences in Wadden Sea eutrophication. Geo-Marine Letters 37: 171-177.

Senent-Aparicio J, Lopez-Ballesteros A, Nielsen A, Trolle D (2021) A holistic approach for determining the hydrology of the mar menor coastal lagoon by combining hydrological & hydrodynamic models. Journal of hydrology 603: 127150.

Servén D, Brummitt C (2018) pyGAM: Generalized Additive Models in Python (v0.4.1). Zenodo. https://doi.org/10.5281/zenodo.1208724.

Sous D, Chevalier C, Devenon JL, Blanchot J, Pagano M (2017) Circulation patterns in a channel reef-lagoon system, Ouano lagoon, New Caledonia. Estuarine, Coastal and Shelf Science 196: 315-330.

Storlazzi CD, Cheriton OM, Messina AM, Biggs TW (2018) Meteorologic, oceanographic, and geomorphic controls on circulation and residence time in a coral reef-lined embayment: Faga'alu Bay, American Samoa. Coral Reefs 37: 457-469.

Sun K, Ren JS, Bai T, Zhang J, Liu Q, Wu W, Zhao Y, Liu Y (2020) A dynamic growth model of *Ulva prolifera*: application in quantifying the biomass of green tides in the Yellow Sea, China. Ecological Modelling 428: 109072.

Taebi S, Lowe RJ, Pattiaratchi CB, Ivey GN, Symonds G, Brinkman R (2011) Nearshore circulation in a tropical fringing reef system. Journal of geophysical research 116: C02016, doi:10.1029/2010JC006439.

Tartinville B, Deleersnijder E, Rancher J (1997) The water residence time in the Mururoa atoll lagoon: sensitivity analysis of a three-dimensional model. Coral Reefs 16: 193-203.

Umgiesser G, Ferrarin C, Cucco A, De Pascalis F, Bellafiore D, Ghezzo M, & Bajo M (2014) Comparative hydrodynamics of 10 Mediterranean lagoons by means of numerical modeling. Journal of Geophysical Research: Oceans, 119(4): 2212-2226.

Viero DP, Defina A (2016) Renewal time scales in tidal basins: Climbing the Tower of Babel. Sustainable Hydraulics in the Era of Global Change: 338-345.

Winter G, Castelle B, Lowe RJ, Hansen JE, McCall R (2020) When is flow re-entrainment important for the flushing-time in coastal reef systems? Continental Shelf Research 206: 104194.

Tables

Table 1: Pearson correlation matrix between offshore wave height (H_s^{ww3}), offshore wave direction (θ^{ww3}), mean wave peak period (T_p^{ww3}), tide (ξ), wind speed (V^{era5}), and wind direction (θ^{era5}).

	θ^{ww3}	T_p^{ww3}	ξ	V^{era5}	θ^{era5}
H_s^{ww3}	0.09	-0.13	-0.01	0.73	0.03
θ^{ww3}		0.32	0.01	-0.14	0.52
T_p^{ww3}			-0.03	-0.32	0.03
ξ				-0.06	0.04
V^{era5}					-0.17

Table 2: Comparative performance of the six GAM models tested in this study to explain the flushing-time of PGD's lagoon (T_f) as a function of offshore wave direction (θ^{ww3}), offshore wave height (H_s^{ww3}), tide (ξ), wind direction (θ^{era5}), wind speed (V^{era5}), and mean wave peak period (T_p^{ww3}). AIC refers to Akaike Information Criterion and ΔAIC to the gain in information provided by the focus model compared to the simpler one. The complexified models were considered supported whenever ΔAIC > 2, following Burnham & Anderson (2002).

Model	Input parameters	AIC	ΔAIC
model 1	θ^{ww3}	9816	-
model 2	θ^{ww3}, H_s^{ww3}	9236	580
model 3	θ^{ww3}, H_s^{ww3}, ξ	9122	114
model 4	θ^{ww3}, H_s^{ww3}, ξ, θ^{era5}	9117	5
model 5	θ^{ww3}, H_s^{ww3}, ξ, θ^{era5}, V^{era5}	9146	-29
model 6	θ^{ww3}, H_s^{ww3}, ξ, θ^{era5}, T_p^{ww3}	9111	6

Table 3: Contribution of the various input parameters (i.e., metoceanic data) into the best GAM model (model 6), which explains the flushing-time of PGD's lagoon (T_f) as a function of offshore wave direction (θ^{ww3}), offshore wave height (H_s^{ww3}), tide (ξ), wind direction (θ^{era5}), and mean wave peak period (T_p^{ww3}). Edf (Effective Degrees of Freedom) refers to the complexity of the smooth functions (see eq. 4).

Parameters	**edf**	**p.value**
Intercept	0.0	1.11×10^{-16}
θ^{ww3}	11.8	3.28×10^{-01}
H_s^{ww3}	8.4	1.11×10^{-16}
ξ	7.7	4.35×10^{-01}
θ^{era5}	5.0	2.45×10^{-01}
T_p^{ww3}	5.5	7.62×10^{-01}

Figure's legends

Figure 1: Study site location and description. a) Location of New Caledonia and the Poé-Gouaro-Déva (PGD) area in the Pacific Ocean. **b)** Satellite snapshot of the PGD lagoon and location of sensors deployed for the purpose of this study.

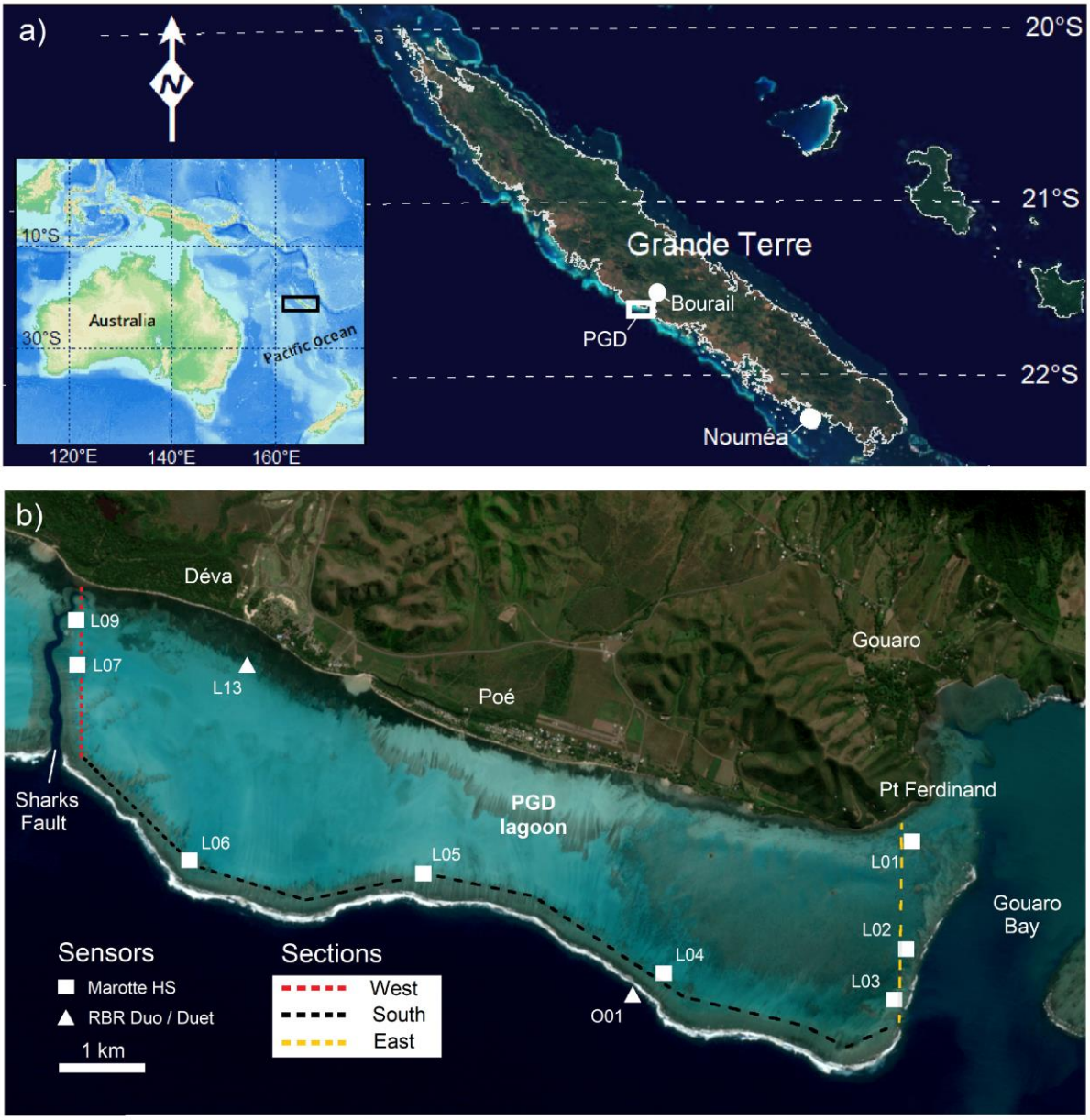

Figure 2: Flowchart summarising the main data sources used and analysis steps implemented in this study. Field raw data are in blue, data used to calculate flushing time (T_f in light green), variables used as input of the GAM model in light yellow, and model output in grey. The flushing time hindcasted over the 2000-2019 was finally used to assess the vulnerability of the lagoon to green tide, taking advantage of the two green tide events that affected the area in 2018 and 2019. Numbers refer to specific steps in the analysis: Field data processing (1); Tidal harmonic decomposition/recomposition (2); Model calibration (3); Model validation with an independent dataset (4); Model prediction to hindcast flushing times over the past decades (5); Cross checking flushing times with dates of green tides that occurred in 2018 and 2019, and comparison with the historical range of flushing times that affected the lagoon to assess its vulnerability to green tides (6).

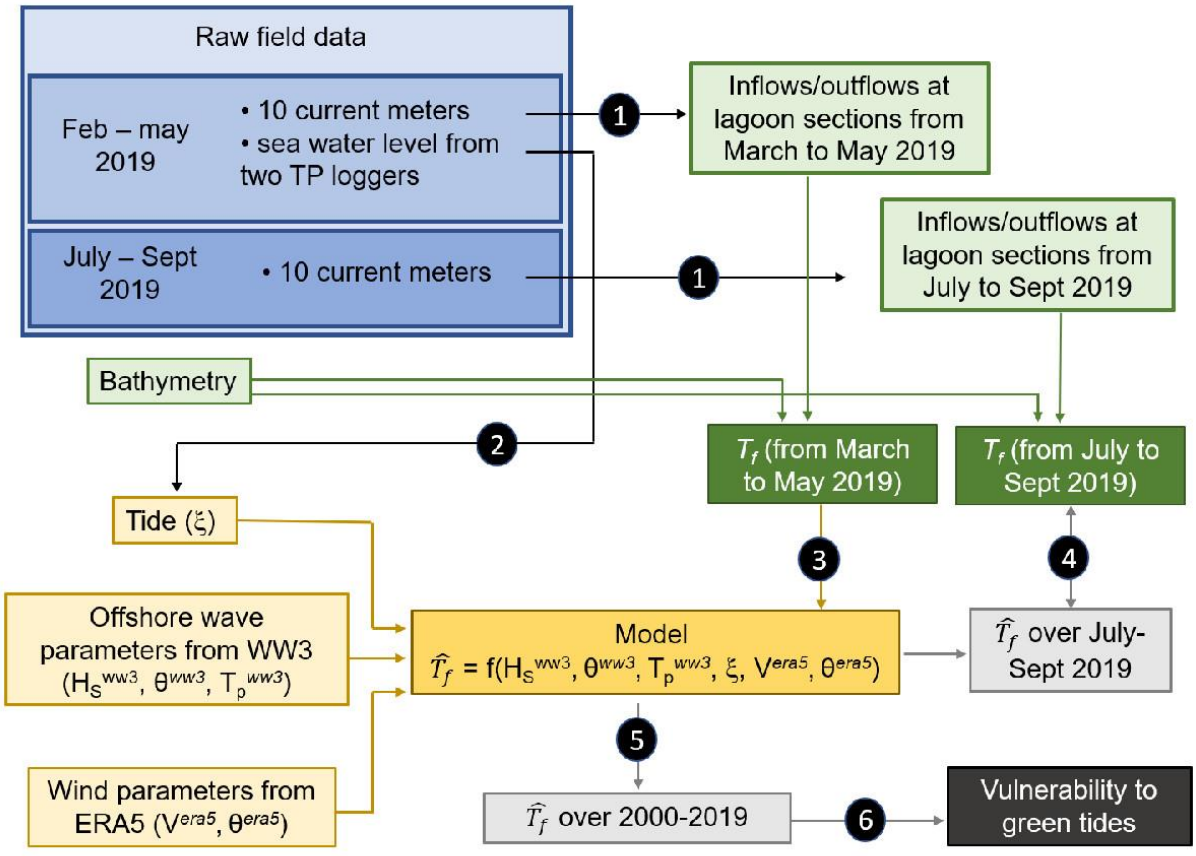

Figure 3: Forcing variables and outflow rate in the PGD area during the first period of measurements. a) Wind speed (V^{era5}, blue line) and direction (black arrows) and mean sea level pressure (green line). **b)** The significant height of offshore wind and swell waves (H_s) from RBR sensor and from WW3, wave direction (θ^{ww3}), wave peak period (Tp) from RBR sensor and from WW3. **c)** Tidal signal (i.e., sea height, ξ) at station O01 and surges of water inside the lagoon (station L13) and on the reef slope (station O01). **d)** Inflow and outflow rates of water measured by the current meters across the east section (water speed averaged over sensors L01, L02, L03), south section (water speed averaged over L05 and L06), and west section (water speed averaged over L07, and L09). Positive mean speed refers to inflow of water from ocean toward the lagoon and *vice versa*. The black dashed line indicates the time period of cyclone Oma influence (from 10 February to 3 March).

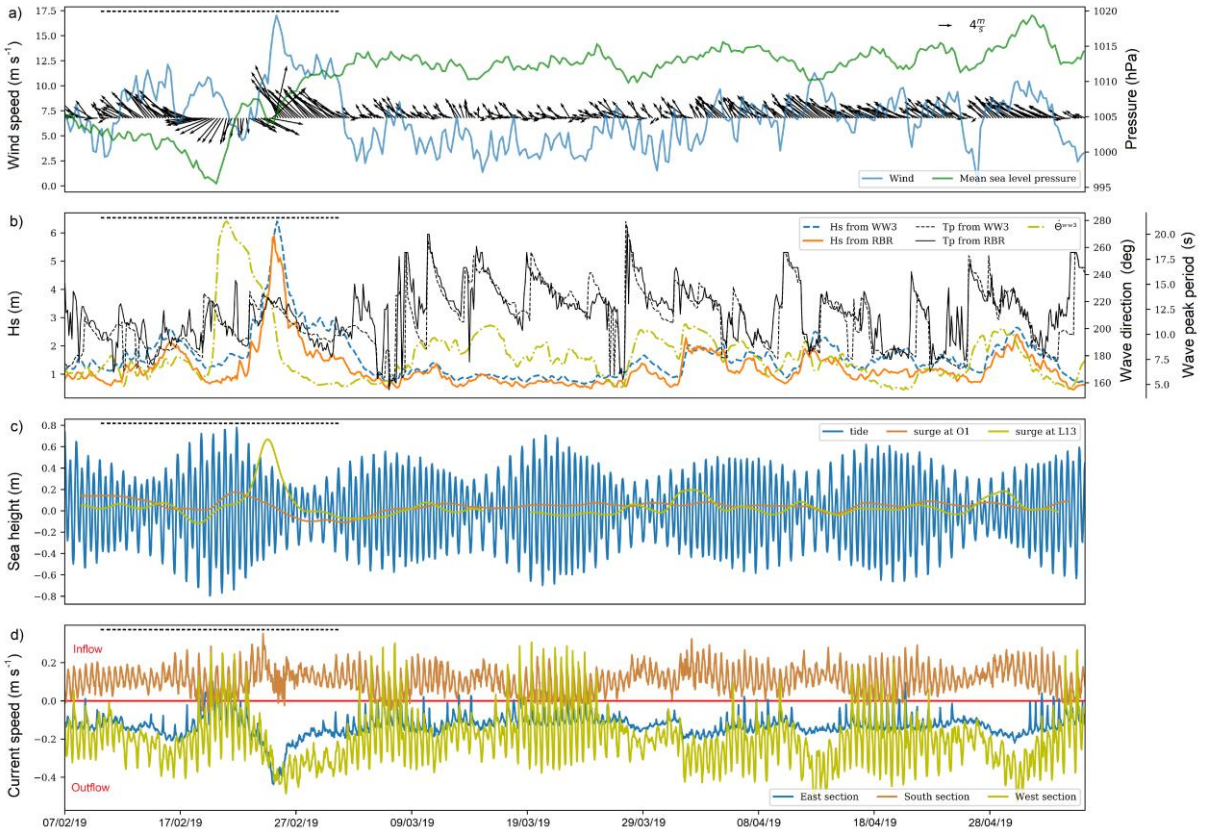

Figure 4: Current speed recorded by loggers as a function of oceanic and atmospheric forcing. a-b) current speed as a function of sea level (tide). Data recorded at rising tide are in red, and at falling tide in blue; **c-d)** current speed as a function of wave height; **e-f)** current speed as a function of wind speed. Left panels **(a, c, e)** are relevant for loggers deployed at the west lagoon section, and right panels **(b, d, f)** for loggers deployed at the east lagoon section. Current speed refers to the mean hourly current, averaged over sensors of the same section. Colours panels refer to wave direction **(c, d)** or wind direction **(e, f)**. Positive speeds (above the red lines) refer to inflows whereases negative speeds (below the red lines) refer to outflows. In each panel, the Pearson's correlation (r) between the variables are provided (upper right corner).

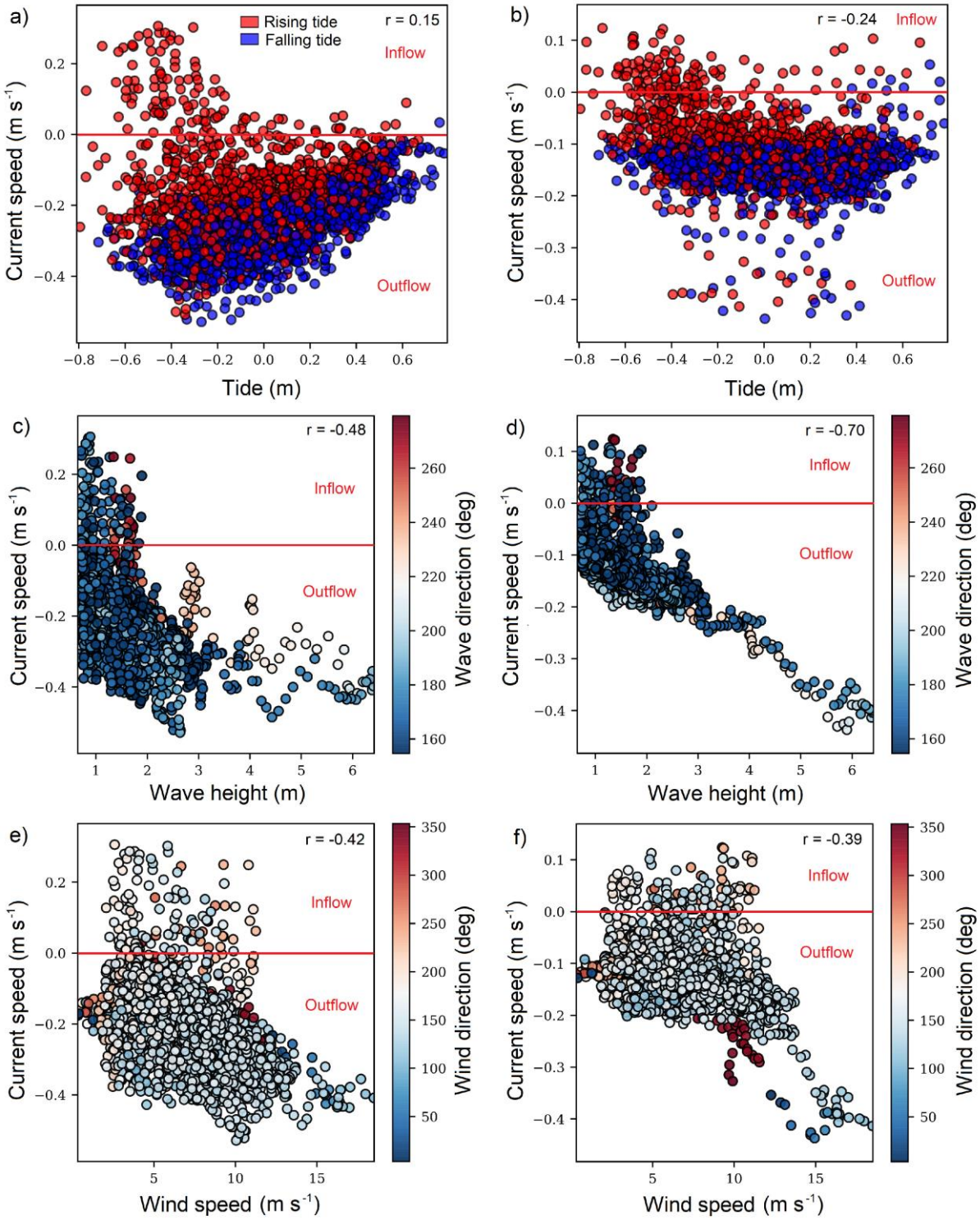
a)
Rising tide
Falling tide
r = 0.15
Inflow
Outflow
Current speed (m s-1)
Tide (m)
b)
r = -0.24
Inflow
Outflow
Current speed (m s-1)
Tide (m)
c)
r = -0.48
Inflow
Outflow
Current speed (m s-1)
Wave height (m)
Wave direction (deg)
d)
r = -0.70
Inflow
Outflow
Current speed (m s-1)
Wave height (m)
Wave direction (deg)
e)
r = -0.42
Inflow
Outflow
Current speed (m s-1)
Wind speed (m s-1)
Wind direction (deg)
f)
r = -0.39
Inflow
Outflow
Current speed (m s-1)
Wind speed (m s-1)
Wind direction (deg)

Figure 5: Performance of Model 6 in predicting the flushing-time of PGD's lagoon. a) Flushing-time calculated from field data (T_f, in green) and modelled from offshore wave, tide and wind, ($\widehat{T}_f$, in black) during the period used for model calibration. The yellow line refers to the difference between T_f and $\widehat{T}_f$.**b)** Same as panel a) but during the second period of measurement, used as independent dataset for model validation purpose. Grey ribbons refer to the 95% confidence intervals.

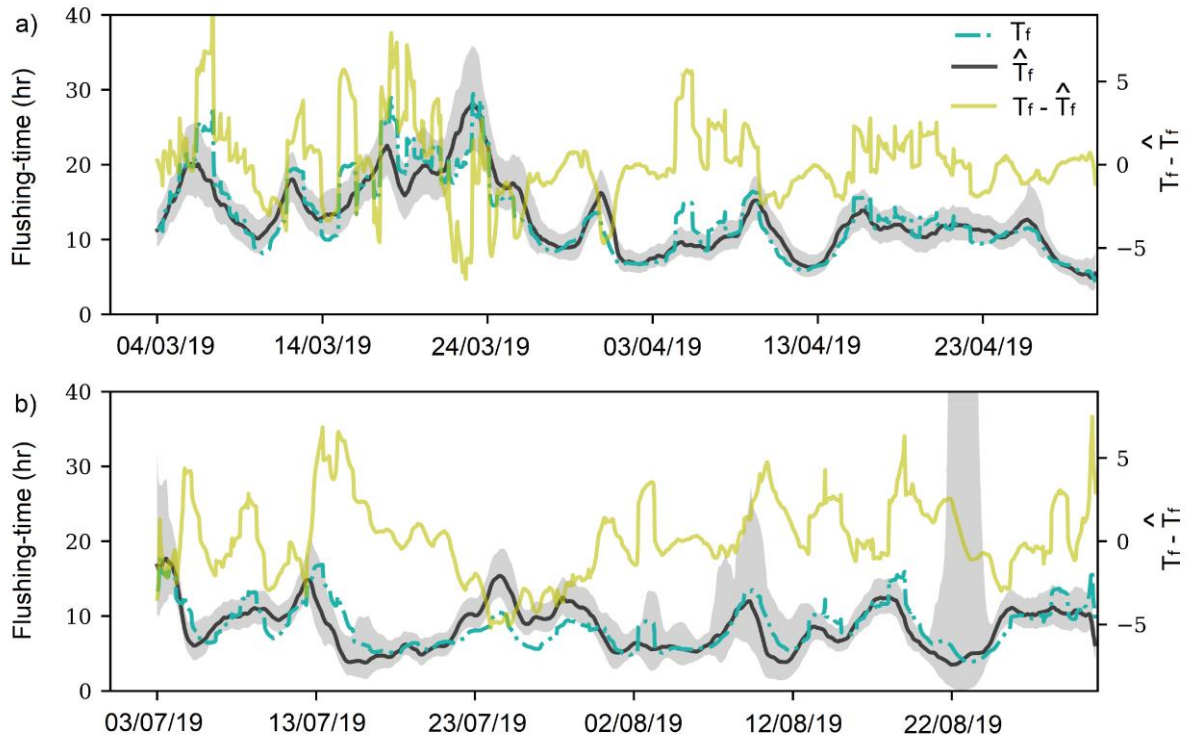

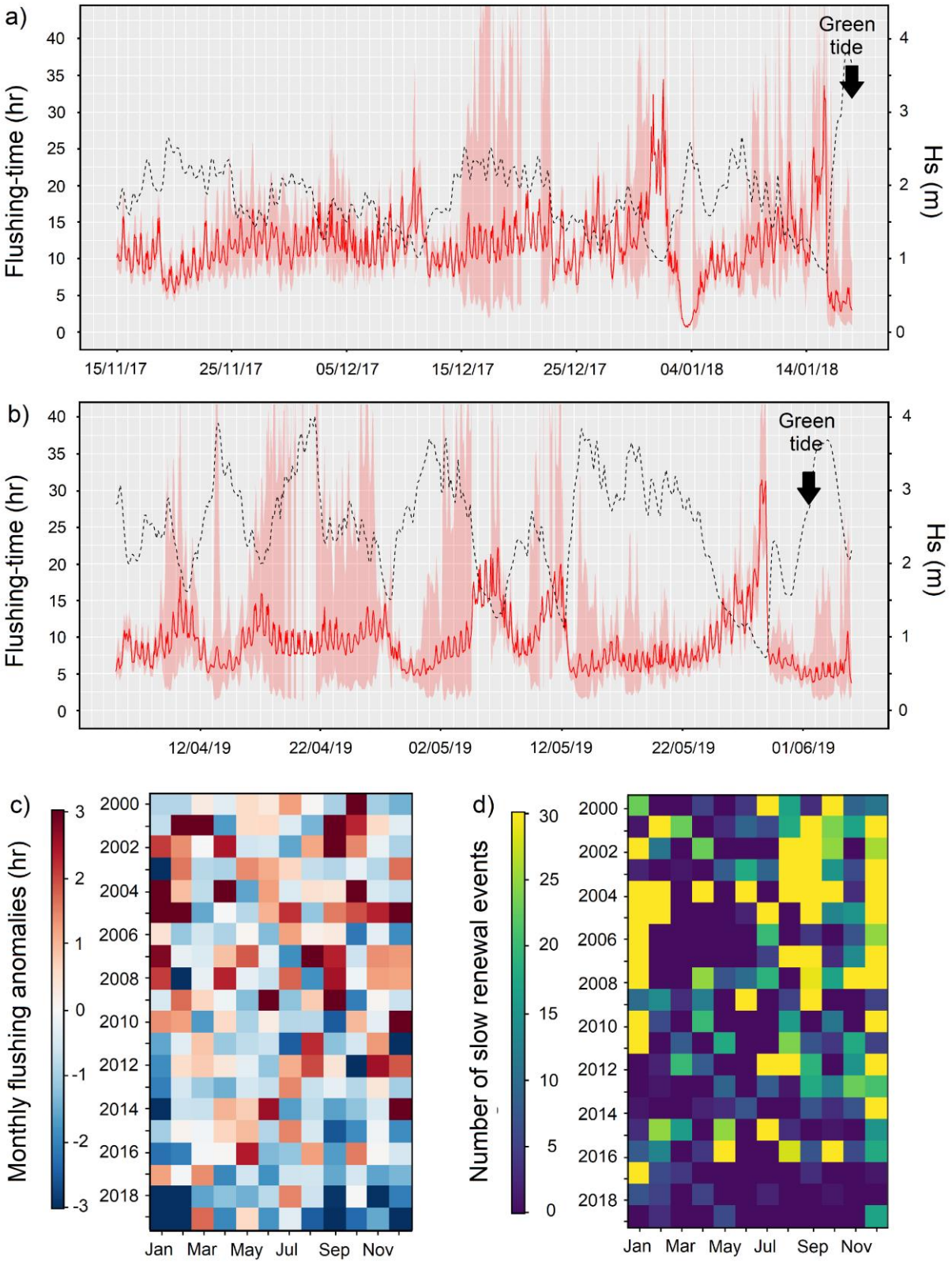

Figure 6: Hindcast of PGD's lagoon flushing-time over the 2000-2019 period. a-b) Hindcasted flushing-time series (red line) before the main green tide that occurred on 18th January 2018 (a) and the one that occurred on 1st June 2019 (b). The shaded red ribbon refers to the 95% confidence intervals around estimates, and the dashed black line refers to the significant wave height Hs (m) from WW3. **c)** Monthly flushing anomalies of the PGD

lagoon from 2000 to 2019. Positive values indicate unusually long flushing-times (i.e., slow renewal of lagoon water). **d)** Number of slow renewal events (i.e., events of long flushing-times) recorded per month, from 2000 to 2019.